Anal. Methods Environ. Chem. J. 8 (3) (2025) 47-61

AMECJ

Research Article, Issue 3
Analytical Methods in Environmental Chemistry Journal
Journal home page: www.amecj.com/ir

# Analysis and evaluation of heavy metals in Rubia tinctorum (L.) as eco-friendly dyes by inductively coupled plasma emission spectrometry and infrared spectroscopy

**EL Jeddaoui Bensalem[a,b,*], Mhamdi Zakya[a], Sabri Mohamed[a], AIT Lyazidi Saadia[b], and Amechrouq Ali[a]**

[a] *Laboratory of Molecular Chemistry and Natural Substances (CMSN), Moulay Ismail University- Faculty of Sciences, Zitoune BP 50000 ,11201 Meknes, Morocco*

[b] *Laboratory of Materials and Archaeomaterials Spectrometry (LASMAR, URL-CNRST, N7°), Moulay Ismail University - Faculty of Sciences, Zitoune BP 50000 ,11201 Meknes, Morocco*

**ARTICLE INFO:**

Received 12 May 2025
Revised form 25 Jul 2025
Accepted 20 Aug 2025
Available online 29 Sep 2025

**Keywords:**
Rubia Tinctorum,
Heavy metal,
Inductively coupled plasma atomic emission spectroscopy,
Infrared spectroscopy,
UV–Vis spectroscopy

**ABSTRACT**

This study investigates the heavy metal composition (Cd, Pb, Fe, Li, Cu, Zn, K, Na, Ca) of Rubia tinctorum (L.) roots collected from Souk Attarine in the historic medina of Fez, Morocco. Thermal analysis (DTA/TGA) revealed significant mass losses within specific temperature ranges. Samples were calcined at 110 °C, 325 °C, 450 °C, and 600 °C. FTIR spectroscopy confirmed the degradation of organic matter and the formation of calcite and silica at higher temperatures. UV–Vis spectroscopy revealed π–π* transitions in the 250–280 nm range and n–π* transitions between 420–550 nm, indicative of alizarin-type chromophores. For elemental determination, samples were acid-digested before analyzed by inductively coupled plasma atomic emission spectroscopy (ICP-AES). The ICP-AES method exhibited excellent linearity ($R^2 > 0.998$) over a concentration range of 0–50 mg $L^{-1}$, depending on the element. Limits of detection (LOD) ranged from 0.003 to 0.066 mg $L^{-1}$, and limits of quantification (LOQ) from 0.010 to 0.083 mg $L^{-1}$, demonstrating high sensitivity and precision. X-ray diffraction (XRD) confirmed the presence of calcite (major peak at 2θ = 29.4°) and secondary quartz in the calcined samples. High levels of essential elements (Ca, K, Fe) and Cd and Pb concentrations below WHO toxicity limits confirm the ecological safety and analytical value of Rubia tinctorum as a natural dye source.

## 1. Introduction

The madder plant (*Rubia tinctorum* L.), a member of the Rubiaceae family, is a perennial climbing species capable of reaching a height of up to 1.5 meters, characterized by its slender, lanceolate, and deciduous leaves [1]. This species is widely recognized as a dye plant, particularly valued in wool dyeing. Additionally, it holds traditional medicinal significance for anemia treatment [2]. The rhizome of madder, which can extend up to 80 cm, is notable for its creeping roots, rich in alizarin, a red anthraquinone compound commonly used as a dye [3]. The cultivation of madder has been successfully established across diverse regions, including the Far East, Europe (notably in France, Italy, and the Netherlands), North America, Mexico, and Africa. Today, the plant has adapted to various areas, including Morocco, where it grows in the wild. Historically, madder has played an essential role in the textile industry as a primary source of red dyes, attributable to the

*Corresponding Author: EL Jeddaoui Bensalem
Email: bensalem.eljeddaoui@edu.umi.ac.ma
https://doi.org/10.24200/amecj.v8.i03.1044

alizarin in its roots [4], but also as a colorant in painting. Such organic dyes could create a wealth of colors, depending on the availability and know-how of resources. These dyes are usually organic in nature, and primarily obtained from different plant sources. Unfortunately, the characterization of natural organic colorants in textiles and artworks is still a challenge. The difficulty of analyzing these materials is sometimes allied to the frequent impossibility of micro-sampling, and the frailty of the objects. Many techniques, such as HPLC (High-Performance Liquid Chromatography. Root yields from plants aged three years can reach between 3 and 5 tons per hectare, allowing the production of approximately 150 to 200 kilograms of dye per hectare [5]. Traditionally, madder has been used to dye carpets and rugs, producing vibrant red shades known as “Turkey Red” [6]. The plant’s capacity to yield long-lasting red and orange hues has rendered it highly valuable over millennia. While the scientific mechanisms underlying this dyeing process are partially understood, ongoing research continues to elucidate specific aspects. Extracting pure dye from madder often requires pretreatment of roots or the application of chemical processes to obtain the dye in its purest form temperature and solvent composition [7, 8]. The use of natural dyes has always been integral, not only in the creation of traditional garments but also in the production of items of sociopolitical significance [9]. Over the centuries, the art of dyeing has evolved alongside societal and artistic advancements, fostering a renewed interest in natural dyes. In recent years, several research studies have investigated the application of sophisticated extraction and preconcentration techniques to enhance the sensitivity and selectivity of analyses for heavy metal content. Some of the extraction methods, such as ultrasound-assisted solid-liquid trap phase extraction with functionalized multi-walled carbon nanotubes (MWCNTs), are very efficient at separating and analyzing nickel content in industrial wastewater [10]. The immobilization of N-acetylcysteine on MWCNTs has also supported the speciation and quantification of manganese (II) and (VII) ions in matrices, including water and biological food matrices [11]. Bimodal mesoporous silica nanoparticles functionalized with amines are used for analyzing lead and calcium content in biological matrices [12, 13]. These materials are finding increasing applications in environmental monitoring, including the removal of mercury vapors [14], and chromium speciation [15], due to their high surface areas and metal ion affinity. These discoveries help the case for the application of ICP-AES, along with thermal and spectroscopic methodologies, to our analysis of *Rubia tinctorum (L.)*. Recent progress made in analytical chemistry has significantly improved both the sensitivity and selectivity of trace metal analysis, especially from biological and environmental matrices. The method based on task-specific ionic liquid-based dispersive liquid-liquid microextraction can accurately measure chromium speciation in whole blood [16]. Likewise, ionic liquid-functionalized multi-walled carbon nanotubes have facilitated efficient speciation and quantification of lead and mercury from environmental and biological liquid media [17, 18]. Geographic Information System (GIS) software has also been used to track pollution by heavy metals in edible vegetables, waters, and soils heavy metals pollutions in waters, soils and vegetables were investigated from farms, near oil refinery in south of Tehran city, Iran (Shahre Ray. Functionalized mesoporous silica nanomaterials are effective at eliminating airborne lead aerosols [19, 20]. Additionally, an overview of analytical techniques for quantifying heavy metals has provided valuable guidance on their practical application [21]. These contributions underscore the necessity of validation, calibration, and method optimization features that underpin the current work.

In this study, we aim to analyze the chemical composition of madder roots using various analytical techniques, including infrared spectroscopy (IR), UV-visible absorption, differential thermal and thermogravimetric analysis (DTA/TGA), X-ray diffraction (XRD), and inductively coupled plasma atomic emission spectroscopy (ICP-AES).

## 2. Materials and Methods

### *2.1. Plant Material*

The roots of madder (*Rubia tinctorum* (L.)) used in this study were sourced from Souk Attarine, a renowned marketplace located in the heart of the ancient medina of Fez, Morocco, known for its diverse selection of plant species, which serve as a key supply for many local artisans. Upon arrival in the laboratory, the roots were carefully sorted to remove any foreign plant material, including stems and roots from other species. The selected roots were then washed thoroughly with water to remove surface debris and dried away from direct sunlight to preserve their chemical constituents. After drying, the roots were ground into a fine powder with an electric grinder. (Fig.1).

### *2.2. Reagents and Chemicals*

All reagents used in this study were of analytical grade. Nitric acid ($HNO_3$, 65%, CAS No.: 7697-37-2), hydrochloric acid (HCl, 37%, CAS No.: 7647-01-0), and hydrogen peroxide ($H_2O_2$, 30%, CAS No.: 7722-84-1) were purchased from Merck (Germany). Potassium bromide (KBr, IR grade, CAS No.: 7758-02-3) for FTIR analysis was also obtained from Merck. Ultrapure deionized water (resistivity >18 MΩ·cm) was used for all dilutions. Standard stock solutions (1000 mg $L^{-1}$) of metals, including Ca, K, Mg, Fe, Zn, Cu, Cd, Pb, and As, were obtained from Sigma-Aldrich and used for calibration of the ICP-AES instrument.

### *2.3. Instrumental and Characterization*

Different instruments, such as infrared spectroscopy, thermogravimetric and differential thermal analysis, UV-Visible absorption, X-ray diffraction (DR-X), and inductively coupled plasma emission spectrometry (ICP-AES), were used to determine heavy metals and characterize Rubia tinctorum (L.). Infrared (IR) spectroscopy was employed as a qualitative analysis technique to identify the principal functional groups in the organic compounds of madder samples. The infrared spectrum, spanning a wavelength range of 4000 $cm^{-1}$ to 400 $cm^{-1}$, enables the measurement of molecular vibrations associated with chemical bonds. Powdered samples were analyzed using a JASCO IFTR 4000 infrared spectrometer. This technique allowed for the detection and identification of characteristic absorption bands corresponding to various functional groups present in the madder extracts. Thermogravimetric analysis (TGA) and differential thermal analysis (DTA) were performed using a DTA 60 analyzer. A 15.3 mg sample of powdered madder root underwent thermal treatment from 25 °C up to 700 °C at a heating rate of 20 °C $min^{-1}$. These analyses facilitated the examination of the thermal stability and decomposition behaviour of the plant sample across this temperature range. The calcination process was conducted to induce chemical

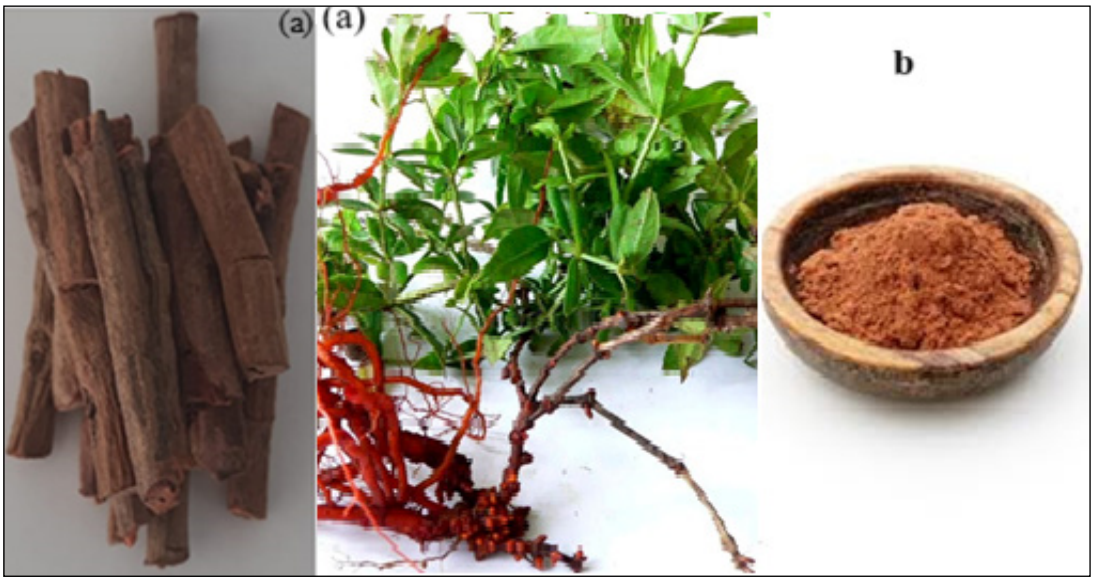


**Fig. 1.** Madder roots (*Rubia tinctorum* (L.)) in (**a**) crushed form and (**b**) powdered form

transformations within the plant samples, leading to their decomposition at high temperatures. Powdered samples were heated in a muffle furnace at three distinct temperatures: 150 °C, 450 °C, and 650 °C. Each temperature was chosen to target specific stages of degradation in the organic and mineral components of the madder roots. The optical absorption spectrum of aqueous madder extracts was measured across a spectral range of 220 to 800 nm. Measurements were carried out using a Jasco V-570 UV/VIS/NIR spectrometer, equipped with a double-window integration sphere (ILN-472). Distilled water was used as the reference in a quartz cuvette, enabling instrument calibration and precise absorption measurements of the various components in the extract. X-ray diffraction (XRD) analysis of calcined madder powder was conducted to determine its mineralogical composition. The XRD measurements of the powder at room temperature were performed using a D8 ADVANCE apparatus equipped with CuKα radiation ($K\alpha_1$ = 1.5418 Å), powered by a 3-kW generator, with a voltage range of 10 to 60 kV and a current range of 5 to 80 mA. Data were collected with a resolution of less than 0.02° at 2θ and a scan rate of 1 second per step from 5° to 80°. Analysis of trace and major elements in calcined madder samples was conducted on an ICP-AES instrument consisting of argon plasma, a cyclonic spray chamber, and a concentric nebulizer. The spectrometer operated sequentially, covering a broad spectrum from 120 to 800 nm, with a resolution of 5 pm between 120 and 320 nm, and 10 pm between 320 and 800 nm. Quantitation was possible on up to 40 elements, supplemented by semi-quantitative evaluations as needed. The sample introduction was performed using an ultrasonic nebulizer and a hydride generator, supported by optional accessories such as a sheath gas system for determining dilute or alkaline solutions and a UV extension kit for halogens. Operating conditions were as follows: the power of the plasma was 1200 W, argon plasma gas flow was 12 $L.min^{-1}$, the flow of the sheath gas was 0.2 $L.min^{-1}$, and the flow of the auxiliary gas was 0.0 $L.min^{-1}$. The instrument enabled the simultaneous analysis of trace and major elements in a wide range of matrices, including saline, organic, and hydrofluoric acid-based samples. The ICP-AES analytical technique is well-known for its sensitivity and accuracy in detecting trace elements, allowing for precise measurement of heavy metal levels in the mineralized extracts of the analyzed samples.

### *2.4. Procedure*

For heavy metal analysis, 0.5 g of dried and powdered *Rubia tinctorum (L.)* root was accurately weighed into a Teflon digestion vessel (Anton Paar Multiwave 3000). A mixture of 10 mL of concentrated nitric acid ($HNO_3$, 65%, Merck, CAS No.: 7697-37-2) and 2 mL of hydrogen peroxide ($H_2O_2$, 30%, Merck, CAS No.: 7722-84-1) was added. The mixture was heated on a hot plate at 120 °C for 90 minutes until complete digestion occurred and a clear solution was obtained. After cooling to room temperature, the digest was filtered using 0.45 µm Whatman filter paper, transferred to a 50 mL volumetric flask, and diluted to volume with deionized water. Following digestion, the solution was analyzed using ICP-AES (Fig. 2a). Also, for IR analysis, a portion of the calcined and ground samples was directly mixed with potassium bromide (KBr, IR grade, Merck, CAS No.: 7758-02-3) in a 1:100 ratio and pressed into pellets under vacuum, as shown in Figure 2b.

## 3. Results and Discussion

### *3.1. Infrared Analysis*

The infrared analysis of *Rubia tinctorum* (L.) root powder in a KBr matrix yielded the spectrum shown in Figure 3. Recent progress made in analytical chemistry has significantly improved both the sensitivity and selectivity of trace metal analysis, especially from biological and environmental matrices. An example is the successful use of task-specific ionic liquid-based dispersive liquid-liquid microextraction to measure chromium speciation in whole blood [16]. Likewise, ionic liquid-functionalized multi-walled carbon nanotubes have facilitated efficient speciation and quantification

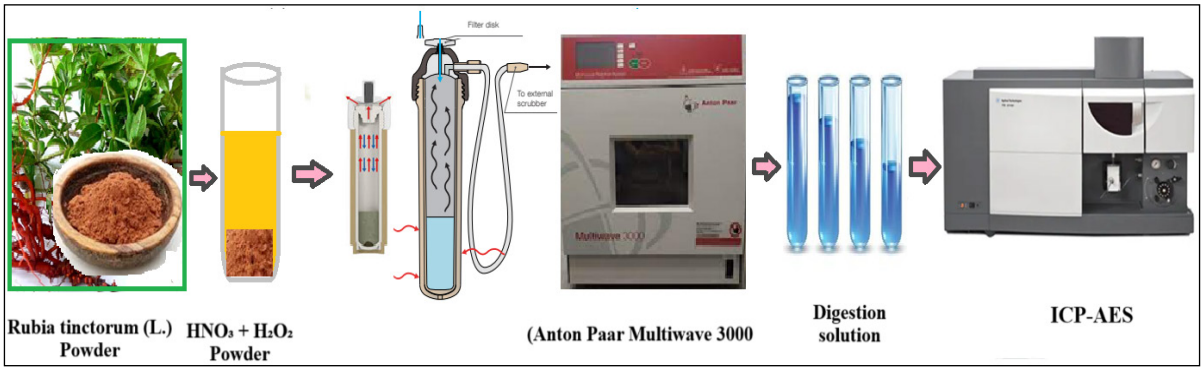


**Fig. 2a.** Sample preparation based on Microwave and analysis by ICP-AES

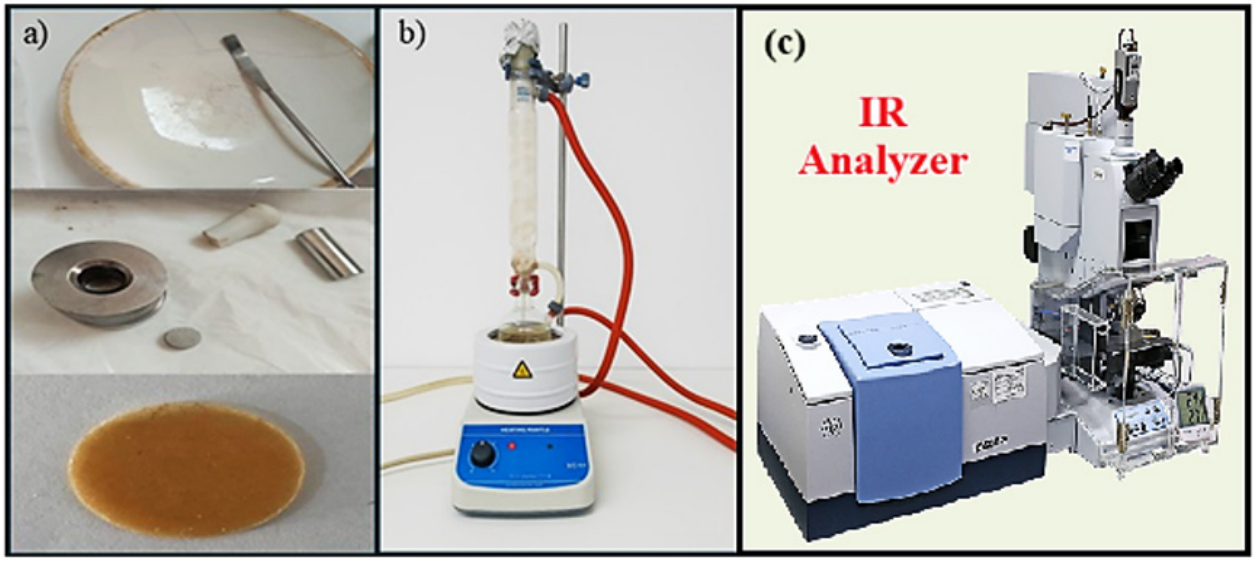


**Fig. 2b.** Experimental set-up used **a**) IR sample preparation, **b**) Mineralization stage, and **c**) IR analysis

of lead and mercury from environmental and biological liquid media [17,18]. Geographic Information System (GIS) software has also been used to track pollution by heavy metals in edible vegetables, waters, and soils [19]. Functionalized mesoporous silica nanomaterials are effective at eliminating airborne lead aerosols [20]. Additionally, an overview of analytical techniques for quantifying heavy metals has provided crucial guidance on their application in real-world settings [21]. These contributions underscore the necessity of validation, calibration, and method optimization features that underpin the current work.

Recent advancements in analytical chemistry have greatly enhanced the sensitivity and selectivity of trace metal detection, particularly in biological and environmental matrices. For instance, dispersive liquid-liquid microextraction using task-specific ionic liquids has been successfully applied for chromium speciation in human blood samples [16]. Similarly, multi-walled carbon nanotubes functionalized with ionic liquids have enabled efficient speciation and determination of mercury and lead in environmental and biological fluids [17,18]. Geographical Information System (GIS) tools have also been employed to monitor heavy metal pollution in edible vegetables, water, and soil [19]. Functionalized mesoporous silica nanoparticles have proven effective in removing airborne lead aerosols [20]. Moreover, a comprehensive review of analytical methods for heavy metal determination has provided critical insights into their application in real-world scenarios [21]. These works emphasize the importance of validation, calibration, and method optimization elements that form the backbone of the present study.

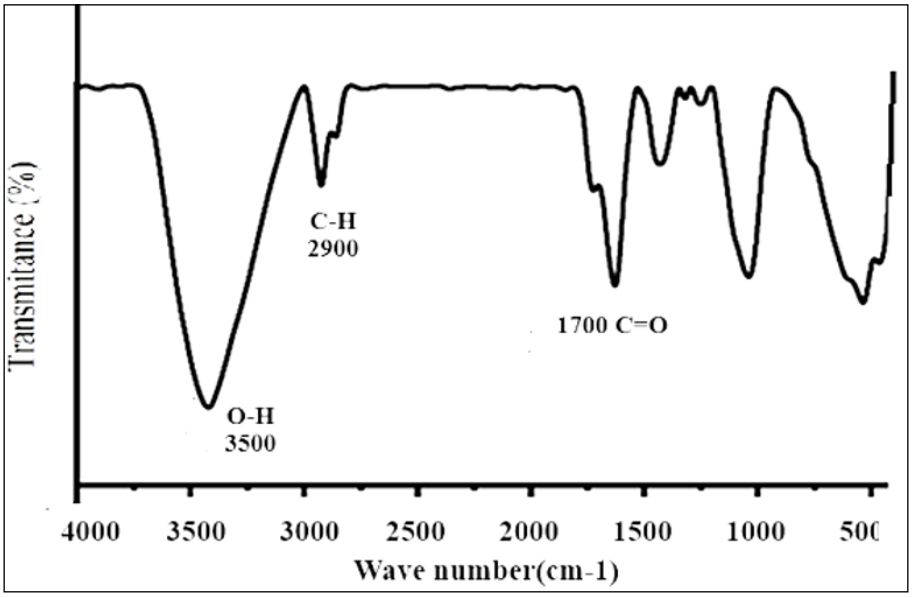


**Fig. 3.** IR Spectrum (KBr) of raw madder powder

The IR spectrum of *Rubia tinctorum* (L.) powder exhibits characteristic spectral features associated with anthraquinones, the primary coloring compounds of the plant. A broad and intense band around 3500 $cm^{-1}$, attributed to the stretching vibration of the hydroxyl group υ(O-H), indicates the presence of hydroxyl groups, which are typical of anthraquinones such as alizarin [23]. Additionally, a band near 2900 $cm^{-1}$ corresponds to the stretching vibration υ(C-H), suggesting the presence of tetrahedral υ(C-H) bonds within the carbon chains [24]. Finally, a sharp band around 1700 $cm^{-1}$ is associated with the stretching vibration of the carbonyl group υ(C=O) in aromatic ketones, confirming the presence of ketone groups consistent with the aromatic structures of anthraquinones[25]. These findings confirm the presence of hydroxyl and ketone functionalities in *Rubia tinctorum* (L.), which aligns with the literature on the chemical composition of this plant and supports its traditional use as a natural dye source.

### *3.2. UV-Vis Analysis*

To further understand the π-π* and n-π* transitions within the previously suggested molecule, we analyzed an aqueous solution of *Rubia tinctorum* (L.) extract using UV-visible spectroscopy. The resulting spectrum is shown in Figure 4.

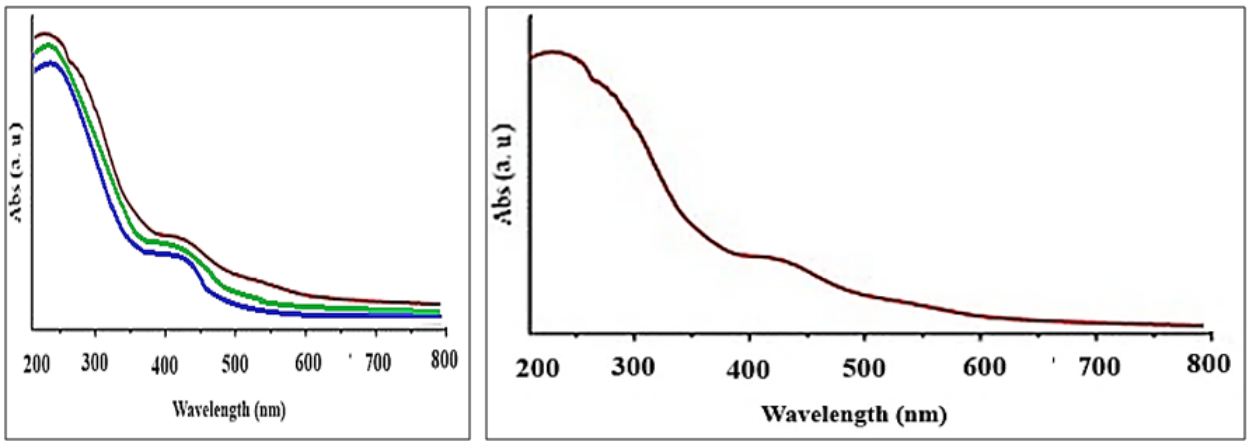


**Fig. 4.** Absorption spectrum of the aqueous solution of madder roots

The spectrum displays distinct absorption bands of the aqueous *Rubia tinctorum* (L.) extract in the ultraviolet region, particularly between λ = 250 nm and λ = 280 nm, which are attributable to the π-π* electronic transitions of the polycyclic aromatic systems in alizarin[26, 27]. In the visible region, significant absorption maxima are observed at approximately λ ≈ 420-440 nm and λ ≈ 500-550 nm. These bands correspond respectively to n-π* transitions and π-π* transitions modified by conjugation with carbonyl groups [28]. These chromophores are responsible for the intense red coloration characteristic of madder. The exact position and intensity of these absorption bands serve as valuable indicators of extract purity, as well as the impact of physicochemical parameters, such as pH and concentration, on the spectral properties of alizarin. These spectral observations align closely with the expected behavior of anthraquinone derivatives in solution [29,30].

### *3.3. Thermogravimetric and differential thermal analysis*

The thermal degradation of the sample is evidenced by a reduction in weight, resulting from both endothermic and exothermic combustion reactions. This transformation process is characterized by thermal degradation occurring in three distinct stages. The initial weight loss of 1.37 mg (8.95%) observed at 150 °C is attributed to the evaporation of water through dehydration and the release of structural water contained within the plant roots. The second stage, occurring at 350 °C, marks the beginning of the thermal degradation of organic matter, resulting in a mass loss of 8.09 mg (52.87%). The third stage, at 650 °C, corresponds to the complete decomposition of organic matter, with an additional weight loss of 4.97 mg (32.48%). The DTA/TGA diagram (Fig. 5) illustrates various degradation reactions, with an endothermic peak at 150 °C attributed to water evaporation, and exothermic peaks at 350 °C and 650 °C associated with the degradation of organic matter.

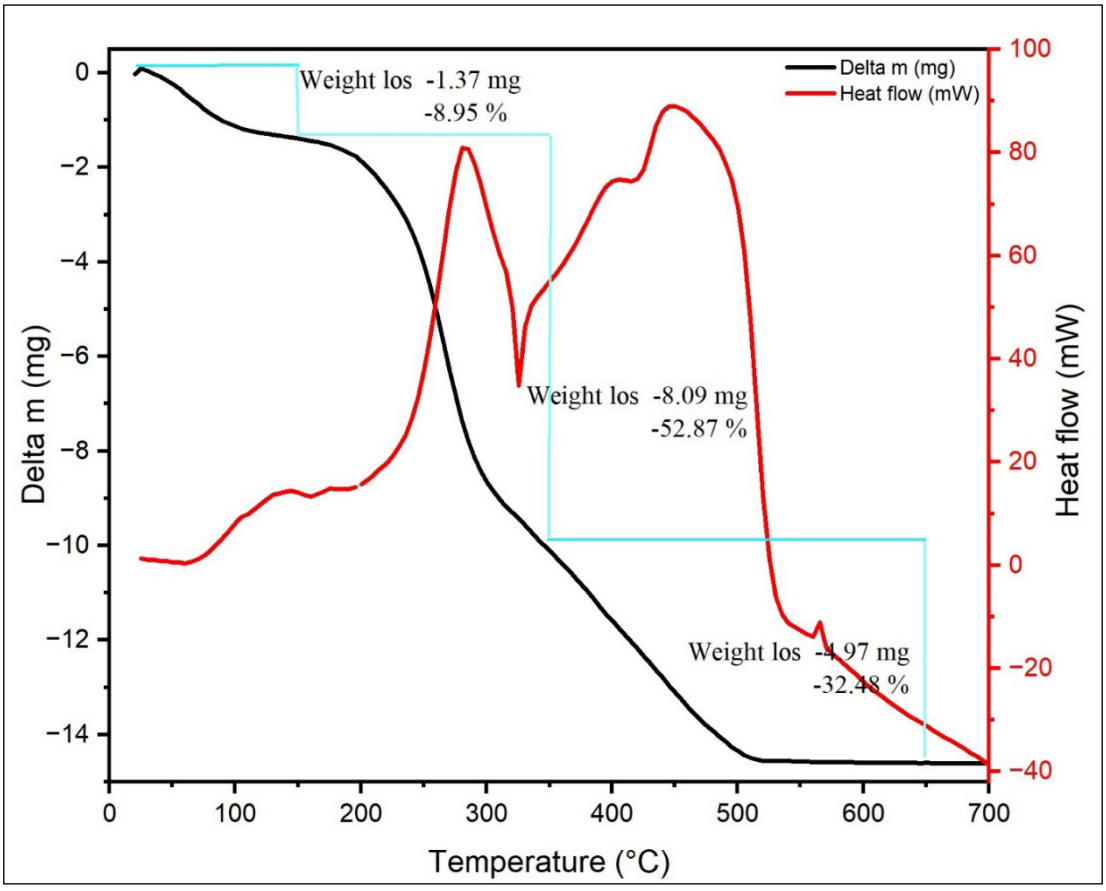


**Fig. 5.** ATD and ATG of the powdered madder roots.

To accurately confirm the mass losses obtained through ATD/ATG analyses, a calcination of powdered roots of the plant *Rubia tinctorum* (L.) was carried out at temperatures close to those of ATD/ATG (150 °C, 350 °C, and 650 °C). The mass losses as well as their percentages are presented in Table 1.

### *3.4. Infrared analysis of madder at different temperatures*

The samples calcined at different temperatures (150 °C, 350 °C, and 650 °C) were compared to the raw product using infrared spectroscopy. The results obtained are presented in Figure 6. The infrared (IR) analysis of *Rubia tinctorum* (L.) samples subjected to different thermal treatments reveals significant modifications in the plant's chemical structure. After the initial thermal treatment at 150 °C, the bands observed at room temperature persist, though their intensity decreases substantially, indicating a slight alteration in the organic functional groups present. At 350 °C, however, the bands associated with organic groups nearly vanish, suggesting the thermal degradation of organic compounds. At this temperature, new bands appear, including those attributed to calcite at 1464 $cm^{-1}$, 871 $cm^{-1}$, and 710 $cm^{-1}$ [31] as well as bands associated with silicon dioxide ($SiO_2$) at 1050 $cm^{-1}$ and 948 $cm^{-1}$ [32,33]. These results align with the literature, confirming the transition from organic components to inorganic compounds at elevated temperatures [34].

**Table 1.** Mass loss after each thermal treatment

| **Powdered madder roots** | | |
|---|---|---|
| Initial mass | 12.00 g | -------- |
| Mass lost after 150 °C | 10.22 g | 10.16 % |
| Mass lost after 350 °C | 11.82 g | 71.83 % |
| Mass lost after 650 °C | 11.07 g | 92.25 % |

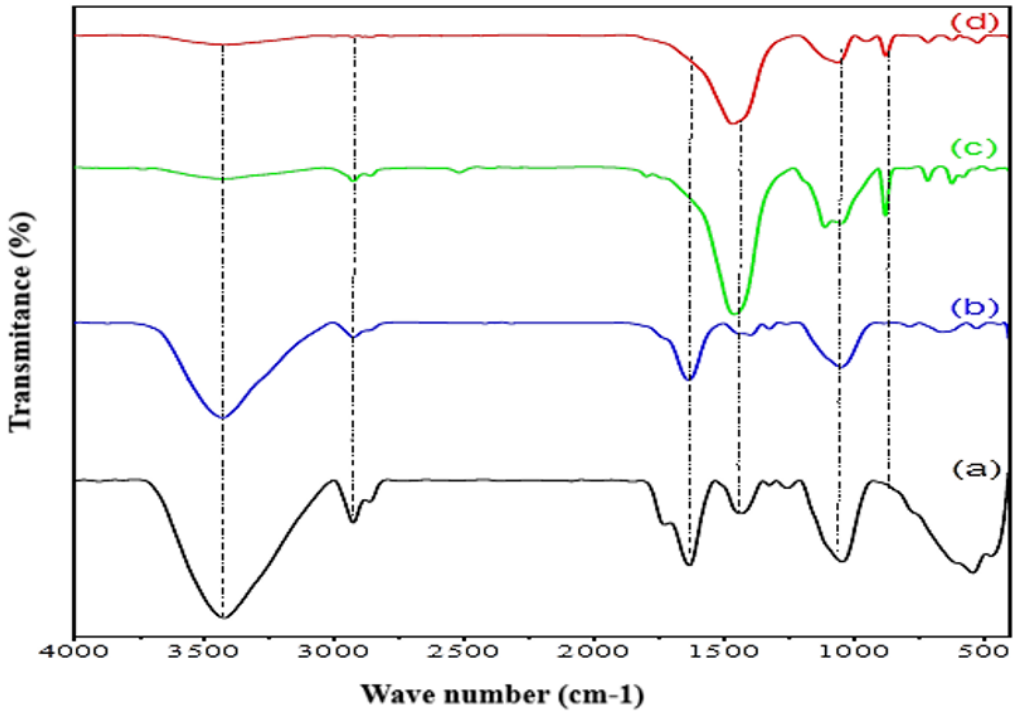


**Fig. 6.** Infrared spectra of raw madder powder at different temperatures [ambient (a), 150 °C (b), 350 °C (c), and 650 °C (d)]

### *3.5. X-Ray Diffraction (XRD)*

After subjecting the plant powder to thermal treatment at 650 °C, an X-ray diffraction (XRD) analysis was conducted. Figure 7 presents the diffractograms of our sample alongside those of calcite and quartz as reference samples [32]. A detailed comparison of the X-ray diffractograms of the unknown sample (black curve) with those of the references (red and green curves) reveals striking similarities in peak positions. These similarities indicate the presence of calcite as a mineral component in the calcined powder, with quartz appearing as a trace element. Distinctive peaks of calcite, such as the one observed at a 2θ angle of 29.4°, corresponding to the (104) crystalline plane[35], as well as additional secondary peaks at 35.9°, 39.4°, and 43.2°, are also evident in the unknown sample[36]. Although the intensity of the peaks in the unknown sample is slightly lower than in the calcite reference, it reflects a significant concentration of calcite. Furthermore, the near-perfect alignment of peaks in both graphs suggests that the crystalline structure of calcite in the unknown sample remains largely intact, with no significant alterations. However, the potential presence of additional or low-intensity peaks may indicate the presence of other mineral phases, notably quartz, within the sample.

### *3.6. Statistical analysis and method validation*

To test the accuracy and reliability of the developed ICP-AES technique for determining heavy metals in *Rubia tinctorum (L.)* root samples, recovery (spiking) tests were performed through a validation experiment. Known concentrations of standard solutions were added to already analyzed samples, then re-analyzed under the same conditions. The elements chosen for validation were Ca, Fe, Cu, Zn, Pb, and Cd, as they have relevance in both the environmental and phytochemical contexts. The range of % recovery, as determined by comparing measured versus expected concentrations, varied from 97.0% to 99.6%, indicating great accuracy. The results for recovery are presented in Table 2. This table summarizes the recoveries for selected elements spiked into previously analyzed madder root samples. Apart from recovery confirmation, the method's overall analytical performance was evaluated. Values for correlation coefficients ($R^2$), detection limits (LOD), quantification limits (LOQ), and the upper linear range for each element were determined. The results, presented in Table 3, verify the high linearity and sensitivity of the ICP-AES method for several analytes.

The table provides emission wavelengths, $R^2$ values of the calibration curve, LOD, LOQ, as well as the upper bounds of the dynamic range for linear detection for every element. The performance criteria and method of validation follow Manousi and Zachariadis (2020)[22], who designed and implemented an equivalent ICP-AES technique for determining trace metals.

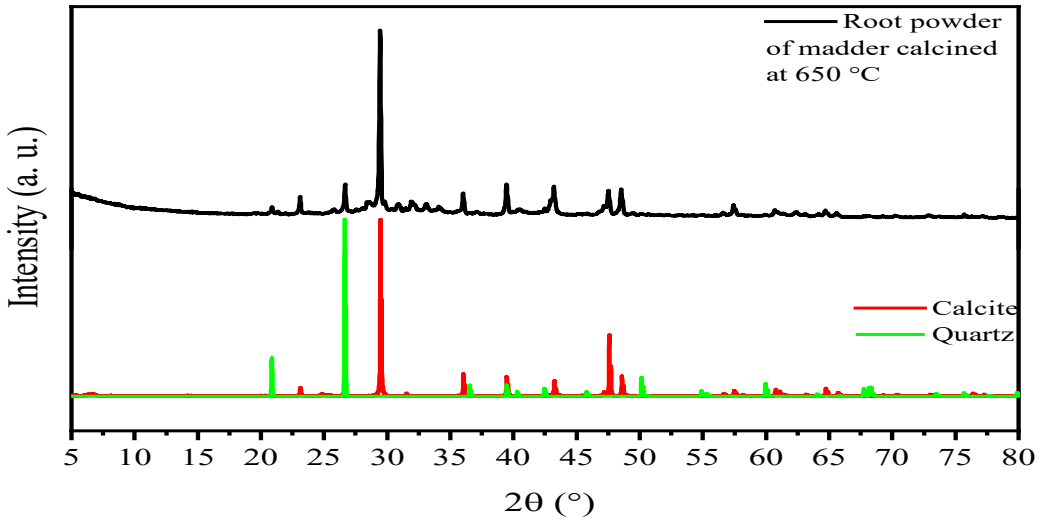


**Fig. 7.** X-ray diffraction spectra of calcined madder roots at 650 °C, calcite, and quartz.

**Table 2.** Recovery values from ICP-AES spiking validation

| Element | Spiked Amount (mg kg$^{-1}$) | Original Content (mg kg$^{-1}$) | Measured After Spiking (mg kg$^{-1}$) | Recovery (%) |
|---|---|---|---|---|
| Ca | 500 | 999.5 | 1492.20 | 98.5 |
| Fe | 50 | 120.3 | 170.10 | 99.6 |
| Cu | 10 | 8.40 | 18.20 | 98.0 |
| Zn | 10 | 12.70 | 22.40 | 97.0 |
| Pb | 5 | 0.92 | 5.88 | 99.2 |
| Cd | 1 | 0.15 | 1.12 | 97.0 |
| Mg | 100 | 80.20 | 179.80 | 99.6 |
| K | 200 | 190.4 | 388.50 | 99.1 |
| Na | 100 | 75.30 | 174.60 | 99.3 |
| Al | 20 | 3.20 | 22.90 | 98.5 |
| Cr | 10 | 0.95 | 10.80 | 98.5 |
| Co | 5 | 0.65 | 5.63 | 99.6 |
| Ni | 5 | 0.78 | 5.67 | 97.8 |
| As | 2 | 0.50 | 2.42 | 96.0 |

**Table 3.** Analytical performance summary of the ICP-AES technique used for elemental analysis of the roots of *Rubia tinctorum (L.)*

| Element | Emission Line (nm) | $R^2$ | LOD (µg g$^{-1}$) | LOQ (mg L$^{-1}$) | Upper Linear Range (mg L$^{-1}$) |
|---|---|---|---|---|---|
| Ag | 328.068 | 0.9989 | 0.0067 | 0.02 | 10 |
| Al | 167.018 | 0.9998 | 0.0033 | 0.01 | 10 |
| As | 188.979 | 0.9999 | 0.0033 | 0.01 | 10 |
| Ba | 230.425 | 0.9995 | 0.001 | 0.003 | 10 |
| Ca | 183.738 | 0.9989 | 0.0037 | 0.011 | 50 |
| Cd | 214.441 | 0.9999 | 0.0033 | 0.01 | 10 |
| Co | 238.892 | 0.9997 | 0.0033 | 0.01 | 10 |
| Cr | 205.571 | 0.9998 | 0.004 | 0.012 | 10 |
| Cu | 324.754 | 0.9997 | 0.003 | 0.009 | 10 |
| Fe | 259.94 | 0.9996 | 0.002 | 0.006 | 10 |
| K | 766.49 | 0.9999 | 0.022 | 0.066 | 50 |
| Mg | 279.078 | 0.9996 | 0.011 | 0.033 | 50 |
| Pb | 220.353 | 0.9987 | 0.0047 | 0.014 | 10 |
| Zn | 213.857 | 0.9999 | 0.001 | 0.003 | 10 |

### *3.7. Analysis of heavy metal Content by the ICP-AES technique*

The roots of *Rubia tinctorum* (L.) are widely used in eco-friendly dyeing of wool and cotton, as demonstrated in previous studies [37]. The chemical purity of this plant, especially the absence of heavy metals and other harmful substances, is crucial to ensuring that the dyeing method remains environmentally sustainable. To verify the absence of these contaminants, a rigorous protocol was applied to the calcined powder at 650 °C, followed by mineralization with concentrated nitric acid. The resulting solution was adjusted to 50 mL with distilled water and filtered using a 0.45 µm Whatman filter paper. The ICP-AES technique subsequently analyzed the filtrate, and the results are summarized in Table 4.

**Table 4.** Heavy metal content in madder roots (mg $kg^{-1}$)

| Elements | Content of Rubia tinctorum (L.) | **WHO [38], [39] |
|---|---|---|
| Ca | > 1000 | ----- |
| K | > 1000 | ----- |
| Mg | 762.31 | ----- |
| Fe | 411.92 | 20 |
| P | 285.87 | ----- |
| Na | 57.383 | ----- |
| Mn | 13.907 | ----- |
| B | 8.8649 | ----- |
| Zn | 4.9035 | 50 |
| Cr | 1.7983 | ----- |
| Cu | 1.467 | 10 |
| Mo | 0.1035 | ----- |
| Cd | 0.1239 | 0.3 |
| As | 0.3013 | ----- |
| Co | < 0.01 | ----- |
| V, Pb | < 0.01 | ----- |

**Normal Content in plants according to WHO ($mgkg^{-1}$)

To ensure the reliability of the analytical method, recovery validation was conducted by spiking known concentrations of selected metals (Ca, Fe, Cu, Zn, Pb, Cd) into the plant matrix. Recovery rates ranged from 97.0% to 99.6%, demonstrating high analytical accuracy and confirming the suitability of the ICP-AES method for quantifying trace and major elements in *Rubia tinctorum* (L.). The analysis revealed that calcium (Ca) and potassium (K) were found in high concentrations, consistent with their role in plant cell wall structure and nutrient regulation [38]. Magnesium (Mg), iron (Fe), phosphorus (P), and sodium (Na) were also abundant, reflecting their involvement in essential physiological processes such as respiration, photosynthesis, and macronutrient assimilation [39]. Regarding toxic heavy metals such as lead (Pb), cadmium (Cd), and arsenic (As), the measured concentrations were below the thresholds established by the World Health Organization [39], thereby confirming the ecological safety of using madder in dyeing applications. Concentrations of cobalt (Co) and vanadium (V) were notably low, below 0.01 mg $L^{-1}$, and nearly undetectable with the instruments employed [40]. A comparative overview of these analytical performance indicators is provided in Table 5. It is also noteworthy that the presence of heavy metals in plants can be influenced by their growth environment, especially in industrial areas where soils may be contaminated with heavy metal deposits, leading to soil degradation [41].

**Table 5**. Comparison with other analytical methods

| Sample | Technique | LOD (mg $L^{-1}$) | LOQ (mg $L^{-1}$) | RSD (%) | Reference |
|---|---|---|---|---|---|
| *Rubia tinctorum* root | ICP-AES | 0.003–0.066 | 0.010–0.083 | <2 | This study |
| Snack food | ICP-AES | 0.18–3.75 µg $g^{-1}$ | 0.6–12.5 µg $g^{-1}$ | <13.5 | [22] |
| Human blood | DLLME + FAAS | 0.45 | 1.5 | 3.8–5.1 | [16] |
| Urine | DSPME + ICP-OES | 0.32 | 1.06 | 4.60 | [13] |

## 4. Conclusion

The consumption of aromatic and medicinal plants holds significant importance in Morocco, raising concerns about potential health risks associated with the accumulation of heavy metals. In this study, a comprehensive characterization of *Rubia tinctorum* (L.) roots was performed using complementary analytical techniques to assess both their chemical safety and their potential as natural dye sources. Thermal analysis (TGA/DTA) revealed the degradation behavior and major mass loss stages of the root material, supporting the structural transitions observed during the calcination process. Infrared spectroscopy (FTIR) indicated the breakdown of organic functional groups and the formation of mineral phases such as calcite and silica at higher temperatures. UV–Vis spectrophotometry showed the presence of chromophoric compounds, particularly alizarin-type pigments, through π–π* and n–π* transitions in the visible range. X-ray diffraction (XRD) further confirmed the formation of crystalline phases, such as calcite and quartz in the calcined samples. In parallel, the validated ICP-AES method was successfully applied to quantify both essential and toxic elements in the plant matrix, revealing low levels of hazardous metals, such as Pb, Cd, and As, all of which were below the WHO guideline values. Although the concentrations were within safe limits, their potential for bioaccumulation over time warrants vigilance. Overall, the findings emphasize the dual role of *Rubia tinctorum* as a safe, eco-friendly dye source and a promising plant for environmental monitoring. Future work should focus on understanding the environmental pathways of metal uptake and enhancing cultivation practices to preserve both the safety and functionality of this culturally significant plant.

## 5. Acknowledgment

The author would like to thank the Laboratory of Molecular Chemistry and Natural Substances and also the Laboratory of Materials and Archaeomaterials Spectrometry, Morocco. This research received no external funding. The authors declare that they have no conflict of interest.

## 6. References

[1] M. N. Navaei, M. Mirza, M. Dini, Chemical composition of the essential oils of Rubia tinctorum L. aerial parts from Iran, Flavour Fragr. J., 21 (2006) 519-520. https://doi.org/10.1002/ffj.1667

[2] K. F. Odounga, Rubia tinctorum L., (El Foua); potentially dangerous medicinal plant: bibliographic update and physicochemical analysis of Moroccan samples, Thèses of Faculty of Medicine and Pharmacy of Rabat., University Mohammed V Faculty DE Medecine ET.DE Pharmacie RABAT, 2011. https://toubkal.imist.ma/handle/123456789/18645

[3] O. Chajii, Ethnobotanical, geographical, phytochemical and dyeing study of the main tinctorial plants in Morocco, Sustain. Chem. Pharm., 36, (2023) 01200. https://doi.org/10.1016/j.scp.2023.101200

[4] P. Nabais, C. Brøns, M. Wozniak, Investigating organic colorants across time: Interdisciplinary insights into the use of Madder, Indigo/woad, and weld in historical written sources, Archaeological Textiles, and Ancient Polychromy, In Textile Crossroads: Exploring European Clothing, Identity, and Culture across Millennia. Zea Books, 2024. https://doi.org/10.32873/unl.dc.zea.1806

[5] R. Lotfi, D. Zakarya, The eco-efficiency of recycling a waste of madder (Rubia tinctorum) vegetable dye, J. Appl. Biosci., 111 (2017) 10877-10881. https://doi.org/10.4314/jab.v111i1.4

[6] U. Dwivedi, Shepherd Textiles, Dyeing with madder root (Rubia Tinctorum), 2024. https://shepherdtextiles.com/dyeing-with-madder-root

[7] G. Cuoco, C. Mathe, P. Archier, F. Chemat, C. Vieillescazes, A multivariate study of the performance of an ultrasound-assisted madder dyes extraction and characterization by liquid chromatography-photodiode array detection, Ultrason. Sonochem., 16 (2009) 75-82. https://doi.org/10.1016/j.ultsonch.2008.05.014

[8] A. D. Pranta, Md. T. Rahaman, Extraction of eco-friendly natural dyes and biomordants for textile coloration: A critical review, Nano-Struct. Nano-Objects, 39 (2024) 101243. https://doi.org/ 10.1016/ j.nanoso. 2024.101243

[9] I. Serafini, A new multi analytical approach for the identification of synthetic and natural dyes mixtures, The case of orcein-mauveine mixture in a historical dress of a Sicilian noblewoman of nineteenth century, Nat. Prod. Res., 33 (2019) 1040-1051. https://doi.org/10.1080/14786419.2017.1342643

[10] M. Dehghani Mobarake, Ultrasound-assisted solid-liquid trap phase extraction based on functionalized multiwall carbon nanotubes for preconcentration and separation of nickel in petrochemical wastewater, J. Anal. Chem., 74 (2019) 865-876. https://doi.org/10.1134/S1061934819090090

[11] J. Rakhtshah, H. Shirkhanloo, M. Dehghani Mobarake, Simultaneously speciation and determination of manganese (II) and (VII) ions in water, food, and vegetable samples based on immobilization of N-acetylcysteine on multi-walled carbon nanotubes, Food Chem., 389 (2022) 133124. https://doi.org/10.1016/j.foodchem.2022.133124

[12] S. Davari Ahranjani, A lead analysis based on amine functionalized bimodal mesoporous silica nanoparticles in human biological samples by ultrasound assisted-ionic liquid trap-micro solid phase extraction, J. Pharm. Biomed. Anal., 157 (2018)1-9. https://doi.org/10.1016/j.jpba.2018.05.004

[13] S. Davari, F. Hosseini, Dispersive solid phase microextraction based on amine functionalized bimodal mesoporous silica nanoparticles for separation and determination of calcium ions in chronic kidney disease, Anal. Methods Environ. Chem. J., 1 (2018) 57-66. https://doi.org/10.24200/amecj.v1.i01.37

[14] F. Golbabaei, A. Vahid, A. Faghihi Zarandi, A novel nano-palladium embedded on the mesoporous silica nanoparticles for mercury vapor removal from air by the gas field separation consolidation process, Appl. Nanosci., 12 (2022) 1667-1682. https://doi.org/10.1007/s13204-022-02366-0

[15] F. Golbabaei, A. Ebrahimi, A. Koohpaei, A. Faghihi-Zarandi, Single-Walled Carbon Nanotubes (SWCNTs), as a Novel Sorbent for Determination of Mercury in Air, Glob J. Health Sci., 8 (2016) 273-280. https://doi.org/10.5539/gjhs.v8n7p273

[16] A. A. M. Beigi, M. M. Eskandari, B. Kalantari, Dispersive liquid-liquid microextraction based on task-specific ionic liquids for determination and speciation of chromium in human blood, J. Anal. Chem., 70 (2015)1448-1455. https://doi.org/10.1134/S1061934815120072

[17] N. Esmaeili, J. Rakhtshah, E. Kolvari, Ultrasound assisted-dispersive-modification solid-phase extraction using task-specific ionic liquid immobilized on multiwall carbon nanotubes for speciation and determination mercury in water samples, Microchem. J., 154 (2020) 104632. https://doi.org/10.1016/j.microc.2020.104632

[18] N. Esmaeili, J. Rakhtshah, E. Kolvari, Rapid Speciation of lead in human blood and urine samples based on MWCNTs@DMP by dispersive ionic liquid-suspension-micro-solid phase extraction, Biol. Trace Elem. Res., 199 (2021) 2496-2507. https://doi.org/10.1007/s12011-020-02382-7

[19] S. A. H. Mirzahosseini, N. Shirkhanloo, S. A. Moussavi-Najarkola, H. Farahani, The evaluation and determination of heavy metals pollution in edible vegetables, water and soil in the south of Tehran province by GIS, Arch. Environ. Prot., 41 (2015) 64-74. https://doi.org/10.1515/aep-2015-0020

[20] A. F. Zarandi, H. Shirkhanloo, P. Paydar, A novel method based on functionalized bimodal mesoporous silica nanoparticles for efficient removal of lead aerosols pollution from air by solid-liquid gas-phase extraction, J. Environ. Health Sci. Eng., 18 (2020)

177-188. https://doi.org/ 10.1007/s40201-020-00450-7

[21] M. Arjomandi, A review: Analytical methods for heavy metals determination in environment and human samples, Anal. Methods Environ. Chem. J., 2 (2019) 97-126. https://doi.org/10.24200/amecj.v2.i03.73

[22] N. Manousi, G. A. Zachariadis, Development and application of an ICP-AES method for the determination of nutrient and toxic elements in Savory snack products after autoclave dissolution, 7 (2020) 66. https://doi.org/10.3390/separations70400662020

[23] E. Ortiz, H. Solis, L. Enrique Noreña, S. Loera-Serna, Degradation of red anthraquinone dyes: Alizarin, alizarin S and alizarin complexone by ozonation, Int. J. Environ. Sci. Dev., 8 (2017) 255-259. https://doi.org/10.18178/ijesd.2017.8.4.958

[24] L. Pronti, Multi-technique characterisation of commercialalizarin-basedlakes,Spectrochim. Acta A Mol. Biomol. Spectrosc., 200 (2018)10-19. https:// doi.org/ 10.1016/ j.saa.2018.04.008

[25] F. Delamare, M. Hovaneissian, Sur deux laques de garance trouvées à Pompei, J. Pompeian Studies, 17 (2006) 39-43. https://www.jstor.org/stable/44291102

[26] C. Clementi, W. Nowik, A. Romani, F. Cibin, G. Favaro, A spectrometric and chromatographic approach to the study of ageing of madder (Rubia tinctorum L.) dyestuff on wool, Anal. Chim. Acta, 596 (2007) 46-54. https://doi.org/10.1016/j.aca.2007.05.036

[27] S. Walki, Microwave assisted structural engineering on efficient eco-friendly natural dye alizarin for dye sensitized solar cells application, Optik, 287 (2023) 171090. https://doi.org/10.1016/j.ijleo.2023.171090

[28] R. Anoua, Optical and electronic properties of the natural Alizarin dye: Theoretical and experimental investigations for DSSCs application, Opt. Mater., 127 (2022) 112113. https://doi.org/10.1016/j.optmat.2022.112113

[29] H. Willemen, G. J. P. Van Den Meijdenberg, T. A. Van Beek, G. C. H. Derksen, Comparison of madder (Rubia tinctorum L.) and weld (Reseda luteola L.) total extracts and their individual dye compounds with regard to their dyeing behaviour, colour, and stability towards light, Color. Technol., 135 (2019) 40-47. https://doi.org/10.1111/cote.12384

[30] M. Yekefallah, F. Raofie, Production of herbal nanocolloids from Rubia tinctorum L. roots by rapid expansion from supercritical solution into suspension system, Ind. Crops Prod., 176 (2022) 114286. https://doi.org/10.1016/j.indcrop.2021.114286.

[31] Z. Mhamdi, M. Sabiri, A. Amechrouq, M. Elhourri, Thermal analysis and determination of the heavy metal content of the plant Urtica Dioica L. by atomic absorption spectroscopy, Int. J. Environ. Sci. Dev., 11 (2023) 44-50. https:// doi.org/ 10.48317/ IMIS T.PRSM/ morjchemv11i1.36577.

[32] V. E. Hamilton, H. Y. McSween, B. Hapke, Mineralogy of Martian atmospheric dust inferred from thermal infrared spectra of aerosols, J. Geophys. Res. Planets, 110 (2005) 2005JE002501. https://doi.org/ 10.1029/2005JE002501

[33] Z. M'hamdi, A. Bouymajane, Chemical composition and antibacterial activity of essential oil of Pelargonium graveolens and its fractions, Arab. J. Chem., 17 (2024) 105375. https://doi.org/10.1016/j.arabjc.2023.105375

[34] J. Götze, Y. Pan, A. Müller, Mineralogy and mineral chemistry of quartz: A review, Mineral. Mag., 85 (2021) 639-664. https://doi.org/10.1180/mgm.2021.72

[35] I. Karmal, S. Mohareb, M. Elhousse, Structural and morphological characterization of scale deposits on the reverse osmosis membranes: Case of brackish water demineralization station in Morocco, Groundw. Sustain. Dev., 11 (2020) 100483. https://doi.org/10.1016/j.gsd.2020.100483

[36] S. Bengamra, M. Oujidi, J. Bastida, V. Esteve-

Cano, Contribution of X-ray diffraction to the determination of mineralogical tracers of particulate atmospheric pollution from a cement plant, Pollut. Atmospherique, 192 (2006) 455-463. https://doi.org/10.4267/pollution-atmospherique.1547.

[37] G. Caliskan, P. Sezgin, E. D. Kocak, S. Altindere, O. Kosemek, Investigation of the dyeability behaviors of cotton surfaces with natural dyes extracted from Rubia Tinctorum and Reseda Luteola L. plants, Mater. Sci. Forum, 1063 (2022) 181-187. https://doi.org/10.4028/p-c30eb5

[38] J. Fliou, Phytochemical screening and analysis of heavy metals of Nerium oleander (L.) leaves, Mediterr. J. Chem., 10 (2020) 346. https://doi.org/10.13171/mjc10402004201366aa

[39] World Health Organization (WHO), Guidelines for assessing the quality of herbal medicines with reference to contaminants and residues, pages 118, 2007. https://www.who.int/publications/i/item/9789241594448

[40] I. Kandić, Heavy metals content in selected medicinal plants produced and consumed in Serbia and their daily intake in herbal infusions, Toxics, 11 (2023) 198. https://doi.org/10.3390/toxics11020198

[41] D. M. Kalonda, A. K. Tshikongo, F. K. K. Koto, C. K. Busambwa, Profile of heavy metals in food plants commonly consumed in some mining areas of Katanga province, J. Appl. Biosci., 96 (2016) 9049-9054. https://doi.org/10.4314/jab.v96i1.2